SCIENCE CHINA
Life Sciences

• RESEARCH PAPER •

October 2018 Vol.61 No.10: 1243–1253
doi: https://doi.org/10.1007/s11427-017-9191-1

BCI induces apoptosis via generation of reactive oxygen species and activation of intrinsic mitochondrial pathway in H1299 lung cancer cells

Jong-Woon Shin[1], Sae-Bom Kwon[1], Yesol Bak[1], Sang-Ku Lee[2] & Do-Young Yoon[1*]

[1]*Department of Bioscience and Biotechnology, Konkuk University, Seoul 05029, Republic of Korea;*
[2]*Targeted Medicine Research Center, Korea Research Institute of Bioscience and Biotechnology (KRIBB), Cheongju 28116, Republic of Korea*

Received September 6, 2017; accepted September 26, 2017; published online March 8, 2018

The compound (*E*)-2-benzylidene-3-(cyclohexylamino)-2,3-dihydro-1H-inden-1-one (BCI) is known as an inhibitor of dual specific phosphatase 1/6 and mitogen-activated protein kinase. However, its precise anti-lung cancer mechanism remains unknown. In this study, the effects of BCI on the viability of non-small cell lung cancer cell lines NCI-H1299, A549, and NCI-H460 were evaluated. We confirmed that BCI significantly inhibited the viability of p53(−) NCI-H1299 cells as compared to NCI-H460 and A549 cells, which express wild-type p53. Furthermore, BCI treatment increased the level of cellular reactive oxygen species and pre-treatment of cells with *N*-acetylcysteine markedly attenuated BCI-mediated apoptosis of NCI-H1299 cells. BCI induced cellular morphological changes, inhibited viability, and produced reactive oxygen species in NCI-H1299 cells in a dose-dependent manner. BCI induced processing of caspase-9, caspase-3, and poly ADP-ribose polymerase as well as the release of cytochrome c from the mitochondria into the cytosol. In addition, BCI downregulated Bcl-2 expression and enhanced Bax expression in a dose-dependent manner in NCI-H1299 cells. However, BCI failed to modulate the expression of the death receptor and extrinsic factor caspase-8 and Bid, a linker between the intrinsic and extrinsic apoptotic pathways in NCI-H1299 cells. Thus, BCI induces apoptosis via generation of reactive oxygen species and activation of the intrinsic pathway in NCI-H1299 cells.

non-small cell lung cancer, apoptosis, BCI, cytotoxicity, anticancer, ROS

Citation: Shin, J.W., Kwon, S.B., Bak, Y., Lee, S.K., and Yoon, D.Y. (2018). BCI induces apoptosis via generation of reactive oxygen species and activation of intrinsic mitochondrial pathway in H1299 lung cancer cells. Sci China Life Sci 61, 1233–1253. https://doi.org/10.1007/s11427-017-9191-1

INTRODUCTION

Lung cancer is a major cause of death worldwide (Siegel et al., 2013) and approximately 75% lung cancer patients die from non-small cell lung cancer (NSCLC) (Jemal et al., 2011). Most cases are diagnosed at advanced, inoperable stages (Pastorino, 2010); although surgery and chemotherapeutics can be employed, most patients eventually succumb to death. Therefore, there is an unmet need for the development of novel chemotherapeutic agents to prolong the survival of patients with NSCLC (Ali et al., 2017).

A tumor is a disease state characterized by uncontrolled cell proliferation and loss of apoptosis. Apoptosis is a genetically programmed and morphologically distinct form of cell death process, which may be triggered by a variety of physiological and pathological stimuli. Apoptosis is executed by distinct mechanisms depending upon the apoptotic stimuli and may be induced by two major pathways: the intrinsic mito-

*Corresponding author (email: ydy4218@konkuk.ac.kr)

chondria-dependent pathway and extrinsic death receptor-dependent pathway (Ali et al, 2017; Liu et al., 2012). To maintain the balance between cell proliferation and death, homeostasis and apoptosis are programmed by our body system. Apoptosis is characterized by cell shrinkage and chromatin condensation and involves a cascade of events, which inactivate critical survival pathways in multicellular organisms. Inhibition of apoptosis may prevent physiological cell death, leading to the development and progression of tumor malignancy (Sipieter et al., 2014; Sankari et al., 2012).

Recent studies have revealed apoptosis as an ideal method for the elimination of cancer cells (Jeong et al., 2010). However, most cancer cells avoid apoptosis through genetic or morphological modifications. Defects in the apoptotic machinery provide a survival advantage to cancer cells and confer resistance to current anticancer therapies. Targeting critical apoptosis regulators is an attractive cancer therapeutic strategy (Lu et al., 2008). Therefore, agents that trigger apoptosis of tumor cells is the current focus of studies related to anti-cancer drug discovery (Xiao et al., 2007).

Many chemotherapeutic agents induce mitochondria-targeted apoptosis. The mitochondria-dependent (intrinsic) pathway is activated from the cell interior in response to severe stress such as DNA or cytoskeletal damage, decreased mitochondrial membrane potential, and transcriptional or post-translation activation of BH3-only pro-apoptotic B-cell leukemia/lymphoma 2 (Bcl-2) family proteins (Ashkenazi, 2008). The decrease in the membrane potential induces the release of apoptotic proteins, including cytochrome c, from the mitochondria into the cytosol (Fulda et al., 2010). Cytochrome c assembles with apoptotic protease-activating factor-1 (Apaf-1) to activate caspase 9. As a consequence, the caspase activates the effector caspases 3, 6, and 7 to carry out apoptosis (Ashkenazi, 2008).

In this study, we assessed the effects of a chemotherapeutic agent (*E*)-2-benzylidene-3-(cyclohexylamino)-2,3-dihydro-1H-inden-1-one (BCI), known as an inhibitor of dual specific phosphatase 1/6 as well as mitogen-activated protein kinase (MAPK) in human lung cancer cells. We demonstrated the effects of BCI on apoptosis through the generation of reactive oxygen species (ROS) and activation of the intrinsic pathway in NCI-H1299 cells.

RESULTS

BCI inhibits tumorigenic proliferation of NCI-H1299 lung cancer cells in a dose-dependent manner

The of BCI on the viability of several cell lines was determined by the 3-(4,5-dimethylthiazol-2-yl)-5-(3-carboxymethoxyphenyl)-2-(4-sulfophenyl)-2H-tetrazolium (MTS) assay. We compared the viability of BCI-treated cells with that of the untreated control cells. Selected lung cancer cell lines (NCI-H1299, NCI-H460, and A549) were treated with various concentrations of BCI for different time periods. As shown in Figure 1, the viability of lung cancer cells decreased in a dose- and time-dependent manner following treatment with BCI (the structure is shown in Figure 1A). The cytotoxic effect of BCI was higher in p53(−) NCI-H1299 cells as compared to NCI-H460 and A549 cells, which express wild-type p53 (Figure 1B–D). A549 and NCI-H460 cells were slightly inhibited by a high concentration of BCI (Figure 1C and D). As the cytotoxic effect of BCI was significant in p53(−) NCI-H1299 cells, we used these cells in subsequent experiments to examine the mechanism underlying BCI-induced apoptosis in lung cancer.

BCI induces morphological changes and apoptosis in NCI-H1299 cells

Features of apoptosis include membrane shrinkage, nuclear fragmentation, and blebbing (Nagata, 2000). Therefore, we evaluated changes in the cell membrane. Phase-contrast microscopy showed that BCI induced cell death and morphological changes in NCI-H1299 cells in a dose-dependent manner following 24-h treatment (Figure 2A). Upon apoptosis induction, the lipid phosphatidylserine (PS) was translocated from the inner to the outer cell membrane via a flip-flop movement. Annexin V, a calcium-dependent protein, is known to bind to PS with high affinity (Sankari et al., 2012). Therefore, we performed annexin V-fluorescein isothiocyanate (FITC)/propidium iodide (PI) staining to evaluate changes in the orientation of PS. Annexin V-FITC/PI staining is generally used to detect apoptosis. In comparison with the control cells, NCI-H1299 cells treated with 1.25–5 μmol L^{-1} BCI for 24 h showed a dramatically increased population of apoptotic cells, indicative of BCI-mediated apoptosis in NCI-H1299 cells (Figure 2B).

BCI increases sub-G_1 population of cells

Cell cycle dysregulation is a major feature of cancer cells. Therefore, we examined whether BCI could regulate cell cycle progression in NCI-H1299 cells. We assessed cell cycle progression by flow cytometry. The sub-G1 population contains hypodiploid fragmented DNA, a distinguishing feature of apoptosis. As shown in Figure 3A and B, BCI-treated NCI-H1299 cells showed increased accumulation in sub-G1 phase as compared with the non-treated control cells. However, BCI treatment failed to show any significant alteration in the expression of factors related to cell cycle, such as cyclin D1, cyclin E, and cyclin A (Figure 3C). Interestingly, the expression level of p21 decreased with an increase in BCI concentration (Figure 3D). As expected, Western blot analysis revealed the absence of p53 expression in p53-knockout NCI-H1299 cells. Together, these results show that BCI dramatically increased sub-G_1 populations but failed to significantly increase cell population in G_0/G_1, S, and G_2 phases.

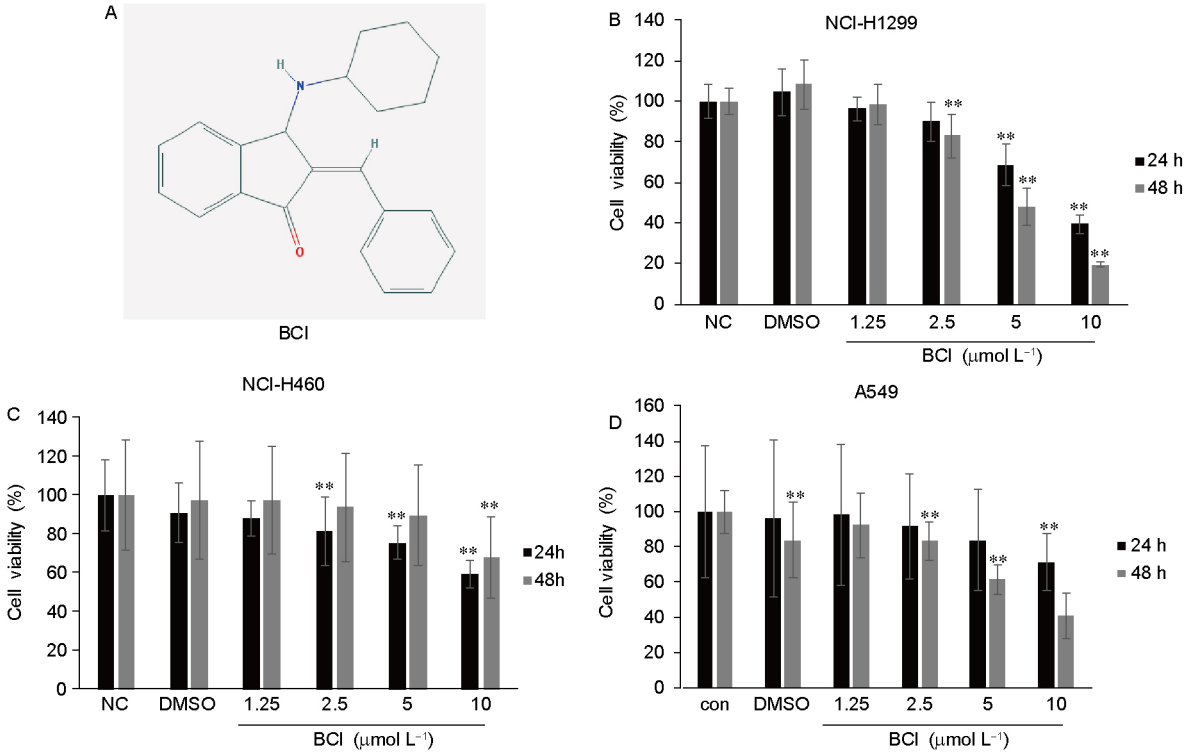

Figure 1 (Color online) Effects of BCI on the viability of human NSCLC cell lines. Cytotoxic effects of BCI on lung cancer cell lines NCI-H1299 (A), NCI-H460 (B), A549 (C) cells were evaluated. These cells were treated for 24–48 h with various concentration of BCI. Cell viability was determined by MTS assay. Data are presented as the mean±SE (n=3). P<0.05 with one-way ANOVA; *, P<0.05, **, P<0.01 with Tukey's HSD test for untreated cells versus BCI-treated cells at indicated concentrations in each cell line.

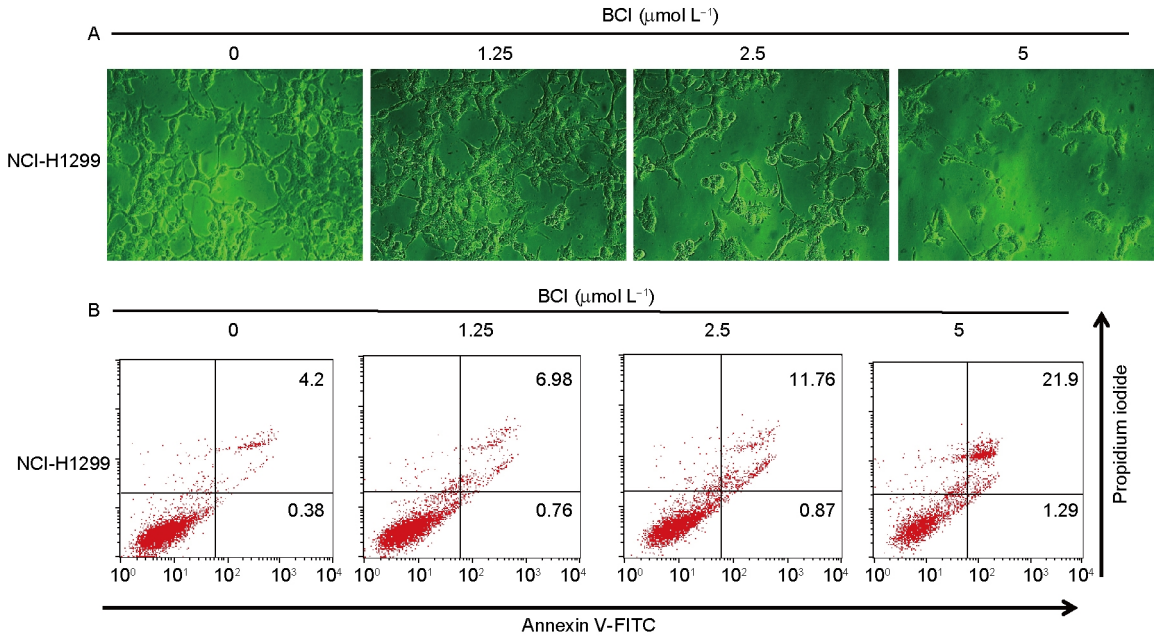

Figure 2 (Color online) Effects of BCI on apoptosis in NCI-H1299 lung cancer cells. A, Microscopic images of NCI-H1299 cells treated with BCI for 24 h. The photographs were taken under phase-contrast microscope at a magnification of 100×. BCI induced morphological changes in NCI-H1299 cells. B, After treatment with the indicated concentrations of BCI for 24 h, NCI-H1299 cells were stained with annexin V-FITC/PI.

BCI activates the intrinsic pathway by regulating Bcl-2 family

Apoptosis is induced through two distinct signaling pathways; the death receptor pathway is typically triggered by ligation of death receptors such as Fas or tumor necrosis factor receptor. These death receptors recruit Fas-associated

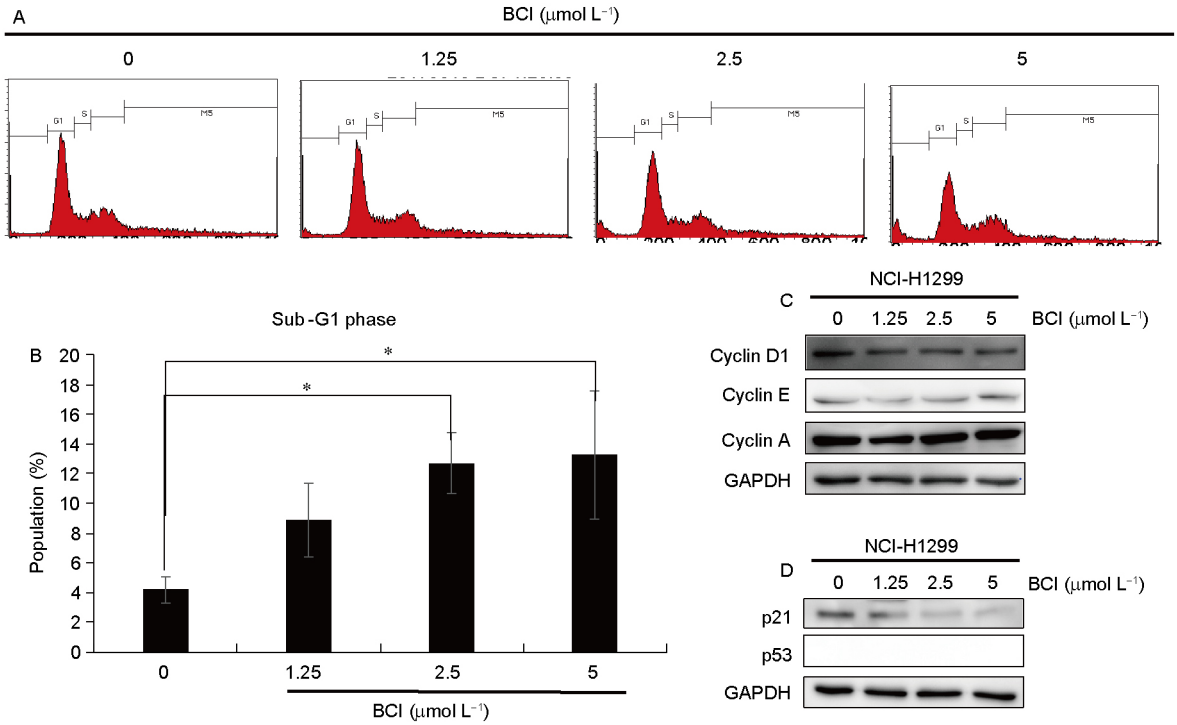

Figure 3 (Color online) Effects of BCI on cell cycle progression in NCI-H1299 lung cancer cells. The cells were treated with 0–5 μmol L^{-1} BCI for 24 h. Following treatment, cells were fixed and stained with PI. A, Cell cycle profiles of BCI-treated NCI-H1299 cells. B, The population of cells in various phases of cell cycle. Data are presented as the mean±SE (n=3). P<0.05 with one-way ANOVA; *, P<0.05, **, P<0.01 with Tukey's HSD test for untreated cells versus BCI-treated cells at indicated concentrations. C, Western blot of cell cycle regulatory factors. GAPDH was used as an internal control.

protein with death domain (FADD) and procaspase-8 to form a death-inducing signaling complex (DISC), leading to the proteolytic activation of caspase-8. Activated caspase-8 may not only directly activate downstream caspase-3 but also cleave Bid to truncated Bid (tBid), which in turn activates the mitochondrial pathway (Li et al., 1998). BCI downregulated or failed to affect the levels of death receptors and their ligands such as DR3, DR5, DR6, FADD, TRAIL, TRADD, and Fas and showed no significant effect on caspase-8 (Figure 4A and B). These data suggest the noninvolvement of the extrinsic pathway in BCI-induced apoptosis. Next, we investigated whether the intrinsic pathway was involved in BCI-induced apoptosis. Mitochondrial dysfunction is the most important factor in the intrinsic pathway. The intrinsic pathway involves the release of mitochondrial cytochrome c into the cytosol. Once released, cytochrome c combines with apoptotic protease activating factor 1 (Apaf-1) and procaspase-9 to form apoptosome in the presence of ATP, resulting in the activation of caspase-9 and caspase-3 (Li et al., 1997). To confirm the important role of Bcl-2 family members in controlling the release of cytochrome c from the mitochondria, we performed Western blot analysis in NCI-H1299 cells. Upon apoptosis induction, the pro-apoptotic protein Bax was activated; in contrast, anti-apoptotic Bcl-2, but not Bcl-xL, was inhibited by BCI treatment in NCI-H1299 cells (Figure 4C). Imbalance in the expression of pro- and anti-apoptotic proteins is associated with cell death (Yang et al., 2003). As the collapse of mitochondria membrane potential (MMP) is a characteristic feature of the intrinsic pathway, the effect of BCI on MMP level was also examined by flow cytometry of JC-1-stained NCI-H1299 cells. While JC-1 aggregation is a feature of healthy cells, apoptotic cells often display JC-1 monomers. As shown in Figure 4D, MMP levels in NCI-H1299 cells treated with various concentrations of BCI were significantly right-shifted compared to those in control cells. Thus, levels of MMP decreased following BCI treatment in NCI-H1299 cells. To further confirm the release of mitochondrial cytochrome c into the cytosol, Western blot was performed using the cytosolic fraction of NCI-H1299 cells. As shown in Figure 4E, cytochrome c was released into the cytosol. Taken together, these results indicate that BCI induced apoptosis via the intrinsic pathway.

Effects of BCI on apoptosis-related factors in NCI-H1299 cells

To further investigate the mechanism underlying BCI-induced apoptosis, we performed Western blot analysis for the evaluation of apoptosis-related factors. A family of cysteine proteases known as caspases mediates apoptosis in mammalian cells (Alnemri et al., 1996). To maintain the apoptotic program under control, caspases were expressed in cells as inactive pro-caspases. During apoptosis, initiator caspases such as caspase-9 and caspase-8 may be activated by cleavage. Furthermore, these caspases cleave the precur-

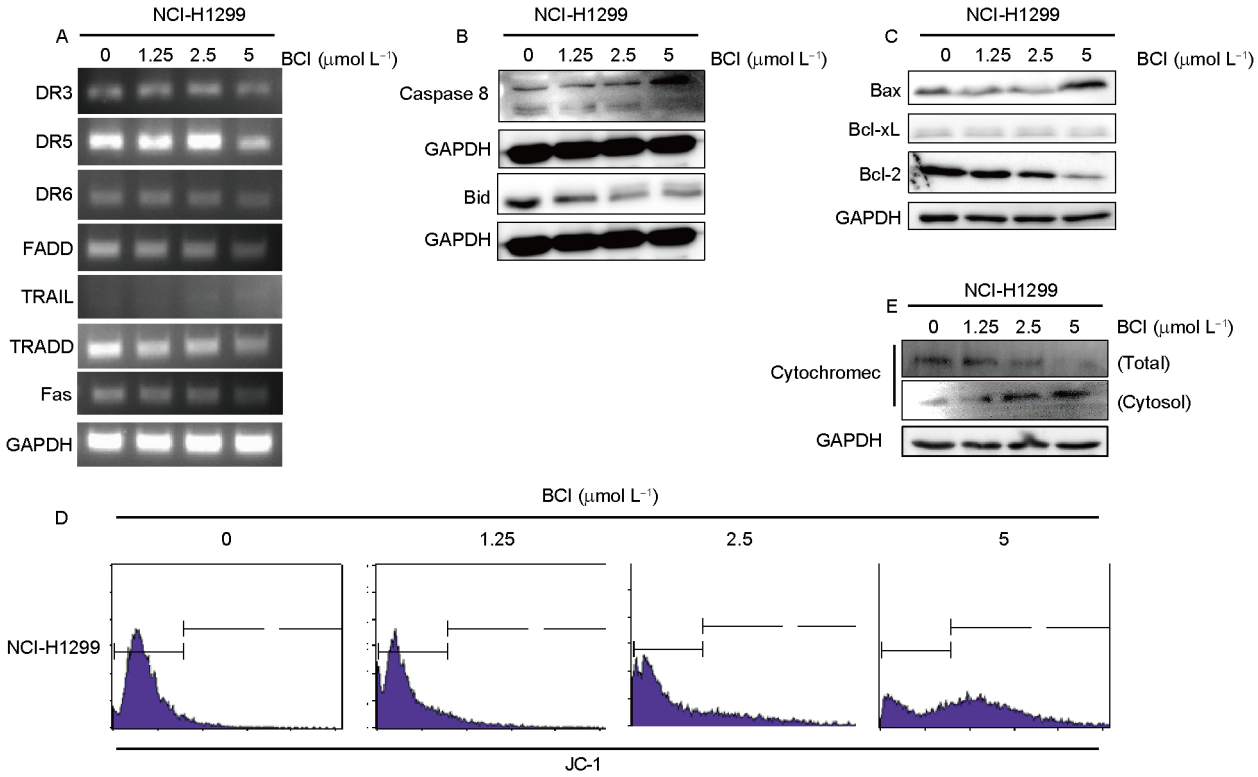

Figure 4 (Color online) Effects of BCI on MMP in NCI-H1299 lung cancer cells. Western blot of cytochrome c was performed using NE-PER. Briefly, 1.5×10^5 NCI-H1299 cells were treated with indicated concentration of BCI for 24 h. A and B, BCI failed to modulate death receptors and extrinsic factors, caspase-8 and Bid. C, Western blot analysis of the pro-apoptotic factors Bax and anti-apoptotic factors Bcl-xL and Bcl-2 in NCI-H1299 cells following BCI treatment. D, Histogram profiles of JC-1 aggregation (FL-1, green) were obtained using flow cytometry. E, Fractionations of NCI-H1299 cells were prepared using NE-PER nuclear cytoplasmic extraction reagent kit (Thermo, USA). Samples were normalized for the protein concentration with the Bradford assay and GAPDH. A total of 50 μg of each cytoplasmic sample was analyzed by Western blot. Cytochrome c release was increased following BCI treatment in a dose-dependent manner.

sor forms of effector caspases such as caspase-6, caspase-7, and caspase-3 (Cryns and Yuan, 1998; Salvesen and Dixit, 1997). In Figure 5A, caspase-9, which forms assembled apoptosome with Apaf-1 and cytochrome c, was cleaved by BCI in NCI-H1299 cells. In addition, BCI treatment increased caspase-3 cleavage, followed by subsequent cleavage of poly ADP-ribose polymerase (PARP) (Figure 5A). The cleaved PARP is a major characteristic of programmed cell death (Alnemri et al., 1996). We elucidated whether BCI would induce apoptosis in NCI-H460 and A549 cell lines, which express wild-type *p53* gene. However, BCI did not induce apoptosis in NCI-H460 and A549 cells (Figure S1 in Supporting Information). In order to confirm whether BCI would induce apoptosis mediated via p53 or not, transfection of *p53* siRNA into NCI-H460 showed no cleaved forms of caspase 3 and PARP, suggesting that BCI induces p53 independent apoptosis (Figure S2 in Supporting Information). To confirm caspase-dependent apoptosis, we performed Western blot analysis using Z-VAD-FMK, a pan-caspase inhibitor. As shown in Figure 5B, pre-treatment with Z-VAD-FMK prevented BCI-induced cleavage of PARP and caspases such as caspase-3 and caspase-9. In summary, these results show that BCI induced caspase-dependent apoptosis.

BCI treatment produces ROS and *N*-acetylcysteine (NAC) reduces BCI-induced apoptotic effects in NCI-H1299 cells

It has been reported that the increase in ROS production may induce caspase activation, resulting in the induction of apoptosis (Han et al., 2017). We investigated the effects of BCI on ROS-related factors by reverse transcription polymerase chain reaction (RT-PCR) and quantitative PCR (qPCR). PCR analyses revealed that superoxide dismutase 2 (SOD2) and catalase, anti-apoptotic and ROS scavenger proteins, were dramatically decreased by BCI in NCI-H1299 cells, while other ROS scavenger proteins such as thioredoxin and peroxiredoxin-1 were unaltered (Figure 6A and B). Furthermore, we used 2′,7′-dichlorofluorescin diacetate (DCF-DA) to investigate ROS production in the presence of BCI and found that the generation of ROS was increased following treatment of NCI-H1299 cells with BCI in a dose-dependent manner (Figure 6C). To investigate whether ROS would affect cell viability, NCI-H1299 cells were pre-treated with NAC (ROS scavenger). In comparison with the BCI-treated group, NAC-treated group showed a dramatic recovery in cell viability. These results suggest that enhanced ROS played an important role in BCI-induced apoptosis.

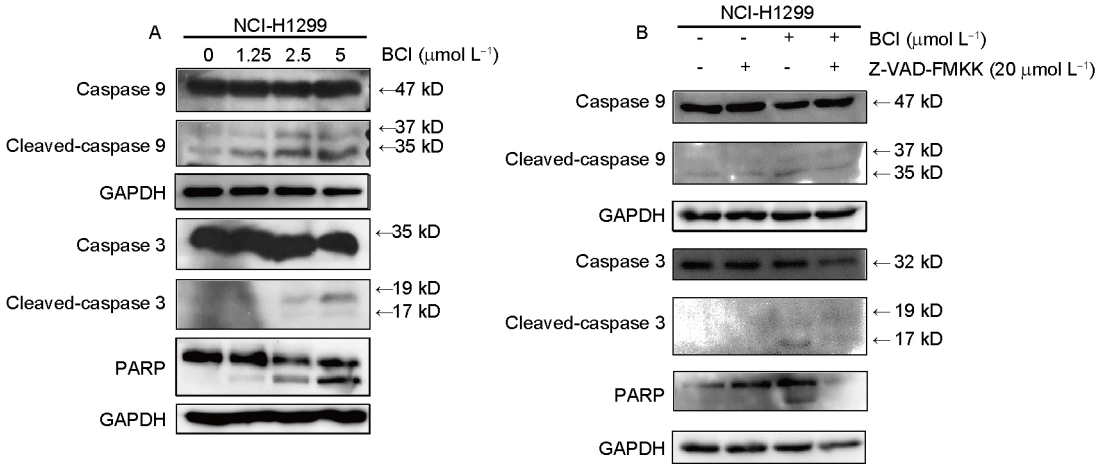

Figure 5 Effects of BCI on apoptosis-related factors in NCI-H1299 cells. NCI-H1299 cells were treated with BCI for 24 h. A, Western blot analysis of caspase 9, caspase 3, and PARP. GAPDH was used as an internal control. B, Effects of caspase inhibitors in BCI-treated NCI-H1299 cells. The cells were pretreated with the pan-caspase inhibitor Z-VAD-FMK (20 μmol L^{-1}) for 3 h, followed by their treatment with BCI for 24 h.

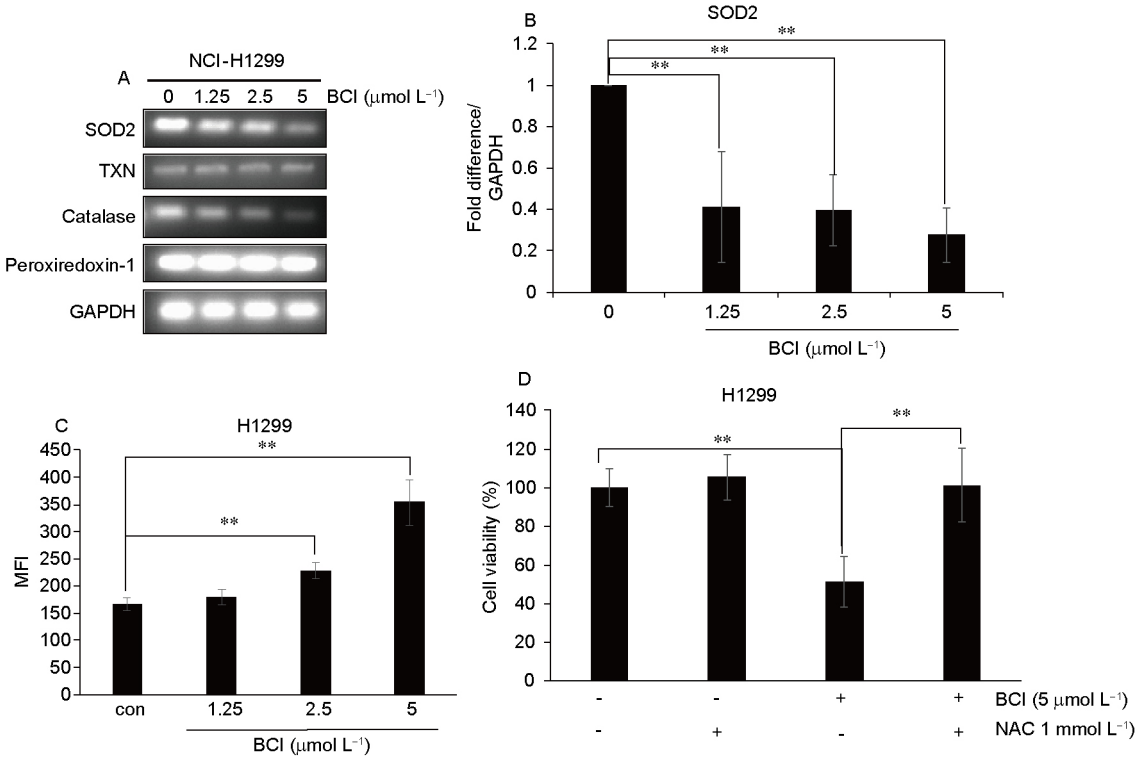

Figure 6 BCI treatment produces ROS and NAC reduces BCI-induced apoptotic effects in NCI-H1299 cells. The cells were treated with BCI for 24 h and the mRNA levels of SOD2 (A and B) and other anti-oxidant enzymes were assessed by RT-PCR. C, BCI treatment resulted in ROS generation in NCI-H1299 cells, as detected by fluorescence microplate reader. D, NAC pre-treatment increased the cell viability. Data were presented as the mean±SE (n=3). P<0.05 with one-way ANOVA; *, P<0.05, **, P<0.01 with Tukey's HSD test for untreated cells versus BCI-treated cells at indicated concentrations.

DISCUSSION

The compound BCI is a cell-permeable cyclohexylamino-indenone that acts as an allosteric inhibitor against MAPK phosphatase activity of dual specificity protein phosphatase (DUSP) 1/6. The phosphorylation of extracellular signal-regulated kinase (ERK) is enhanced in HeLa cells overexpressing human DUSP1 and DUSP6. BCI blocks DUSP6 activity and enhances the expression of target genes of fibroblast growth factor in Zebrafish embryos. *In vitro* studies support a model, wherein BCI inhibits DUSP6 catalytic activation by ERK2 substrate binding (Molina et al., 2009). How BCI induces apoptosis in lung cancer cells is, however, still questionable. Therefore, we evaluated the mechanism underlying BCI-mediated apoptosis.

The main purpose of our study was to confirm the anti-cancer effect and associated mechanisms of BCI in human

lung cancer cells. We investigated the anti-cancer effects of BCI in NCI-H1299 cells and found that BCI inhibited tumor growth by ROS generation and induced apoptosis in NCI-H1299 cells in a dose-dependent manner via caspase activation and PARP cleavage (Figures 2A and 5A and B). As shown in Figure 1A–C, the anti-cancer effect of BCI was higher in NCI-H1299 cells as compared to NCI-H460 and A549 cells, which express wild-type *p53* gene. Hence, we used NCI-H1299 cells for the subsequent experiments. We investigated whether p53 plays essential roles in the cytotoxic effect of BCI. NCI-H460 and A549 cells were transfected with *p53* siRNA, followed by their treatment with BCI for 24 h. BCI had no effect on p53(+) lung cancer cells transfected with p53 siRNA (Figure S2 in Supporting Information) (Bak et al., 2011). These results demonstrate that p53 played no role in BCI-induced cytotoxicity, suggestive of the involvement of other factors in BCI-induced cytotoxicity. In addition, we evaluated the cytotoxic mechanism of BCI against NCI-H1299 cells. Previous studies have indicated that oxidative stress plays an important role in regulating apoptosis in tumor cells. Apoptosis may be induced by chemotherapeutic agents via enhancement in ROS generation and perturbation of redox homeostasis (Dixit et al., 2009; Dixit et al., 2014).

Apoptosis is induced by two major pathways: intrinsic and extrinsic pathways. The intrinsic pathway is associated with mitochondrial membrane permeabilization and cytochrome c release from the mitochondria into the cytosol (Kroemer et al., 1998; Mignotte and Vayssiere, 1998). In the cytosol, cytochrome c assembles into the apoptosome with Apaf-1 and caspase-9. The activated caspase-9 is an effector caspase (Rodriguez and Lazebnik, 1999). The extrinsic pathway receives signals through the binding of the extracellular receptor ligand to pro-apoptotic death receptors located on the cell surface (Ashkenazi and Dixit, 1998). Death receptors along with the ligand form DISC composed of death receptor, FADD, and caspase-8 (Kischkel et al., 1995). These DISCs promote a downstream signaling cascade, resulting in apoptosis induction (Algeciras-Schimnich et al., 2003; Lavrik et al., 2005; Wilson et al., 2009). The imbalance between anti-apoptotic proteins such as Bcl-xL and Bcl-2 and pro-apoptotic proteins such as Bax and Bad determines the fate of cells (van Gurp et al., 2003). Mitochondria play an important role in death signal amplification and transduction of the apoptotic response. An important role of mitochondria in apoptotic signaling is to translocate cytochrome c from the mitochondrial inner membrane into the cytosol. Upon its release, cytochrome c together with Apaf-1 activates caspase-9, which in turn activates caspase-3 (Kroemer and Reed, 2000). The release of cytochrome c and cytochrome c-mediated apoptosis is regulated by Bcl-2 family members such as Bcl-2 and Bax, which are important regulators. In response to a variety of anticancer drugs, Bax translocates to the mitochondria and binds to the mitochondria membrane, allowing the release of cytochrome c (Li et al., 2012). However, Bcl-2 prevents cytochrome c efflux by binding to the mitochondria membrane and forming a heterodimer with Bax, resulting in the neutralization of pro-apoptotic effects (Huang et al., 2006). Thus, the balance between Bcl-2 and Bax is important for determining cell fate, including survival and death. We found that BCI treatment increased the ratio of Bax/Bcl-2. These results may be important in BCI-induced apoptosis.

The process of BCI-induced apoptosis involved activation of caspase-3 and caspase-9, and treatment with a pan-caspase inhibitor markedly prevented BCI-induced cell apoptotic effects. Therefore, BCI-induced apoptosis depends on the activation of caspases, in particular, caspase-3 and caspase-9 (Figure 5B). However, BCI treatment failed to promote activation of caspase-8 or its upstream molecules such as FasL and Fas. Taken together, BCI activates apoptosis through the intrinsic pathway but not the extrinsic pathway. Apoptosis and cell cycle arrest are considered as the major reasons for the inhibition of cell proliferation (King and Cidlowski, 1998). During cell division, the cells in G_2/M phase contain more DNA than those in G_0/G_1 phase. Cells in Sub-G_1 phase have hypodiploid fragmented DNA, which is an important marker of apoptosis (Karna et al., 2011). Cyclins such as cyclin D1, A, and E promote cell cycle progression. Moreover, each cyclin is involved in a specific phase of the cell cycle (Evans et al., 1983). PI is an intercalating agent that can penetrate the cell membrane of only dead cells, thereby distinguishing these cells from the living cells (Moore et al., 1998). Our results suggest that BCI treatment failed to induce cell cycle arrest but increased sub-G_1 populations in NCI-H1299 cells. To determine whether BCI induces cell death, we performed the annexin V-FITC/PI staining. Apoptosis induction results in the flip-flop of lipid molecules on the surface of the cell, followed by the binding of annexin V to the cell surface (Vermes et al., 1995). BCI-treated cells showed significant level of apoptosis compared to untreated cells.

In conclusion, BCI has significant anti-cancer effects against lung cancer cells and increases sub-G_1 populations in NCI-H1299 cells (Figure 3A and B). BCI enhanced ROS level and induced an imbalance in Bcl-2 family proteins such as Bcl-2, Bax, and MMP, leading to apoptosis via the intrinsic pathway (Figure 6).

Taken all data, BCI enhanced the level of cellular reactive oxygen species, and also inhibited anti-oxidant enzymes such as SOD2 and catalase in NCI-H1299 cells. BCI induced processing of caspase-9, caspase-3, and poly ADP-ribose polymerase as well as the release of cytochrome c from the mitochondria into the cytosol. In conclusion, BCI induces apoptosis via generation of reactive oxygen species and activation of the intrinsic pathway such as downregulation of Bcl-2 expression and enhanced Bax in NCI-H1299 cells. This is the first study to demonstrate the molecular mechanism of BCI-me-

diated inhibition of lung cancer cell proliferation. Thus, BCI may serve as a potential therapeutic agent for the treatment of human lung cancer (Figure 7).

MATERIALS AND METHODS

Reagents

The stock solution of BCI (200 mmol L^{-1}) in dimethyl sulfoxide (DMSO) was stored in the dark at 4°C and diluted in Roswell Park Memorial Institute (RPMI)-1640 medium immediately before use. CellTiter 96 AQueous One Solution Cell Proliferation Assay Reagent (MTS) was purchased from Promega (USA) and PI, from Sigma-Aldrich (USA). NE-PER nuclear and cytoplasmic extraction reagents were obtained from Pierce (USA). Antibodies specific to PARP, caspase-3, caspase-8, caspase-9, p53, Bcl-2, Bcl-xL, Bax, Bid and cytochrome c were procured from Cell Signaling Technology (USA). The anti-rabbit IgG horseradish peroxidase (HRP)-conjugated secondary antibody, anti-mouse IgG HRP-conjugated secondary antibody, and BCI were supplied by Millipore (USA). Antibodies specific to p27, p21, and glyceraldehyde 3-phosphate dehydrogenase (GAPDH) were purchased from Santa Cruz Biotechnology (USA). JC-1 (5,50,6,60-tetrachloro-1,10,3,30-tetraethyl benzimidazolylcarbocyanine chloride) was obtained from Enzo (USA). General caspase inhibitor Z-VAD-FMK was supplied by R&D Systems (USA) and the FITC-Annexin V apoptosis detection kit I, by BD Biosciences (USA). DCF-DA was procured from Abcam (UK) and siRNA p53, from ST Pharm (Korea).

Cell lines

Human NSCLC cell lines, including human lung adenocarcinoma cell line A549, human lung adenocarcinoma cell line NCI-H1299, and human large cell lung carcinoma cell line NCI-H460, were purchased from the American Type Culture Collection (USA). Cells were cultured in RPMI medium (Korea) containing 10% (v/v) heat-inactivated fetal bovine serum (USA). Cells were incubated at 37°C in an atmosphere of 5% CO_2/95% air with saturated humidity.

Cell viability assays

Cell viability was assessed by the MTS dye reduction assay, which measures mitochondrial respiratory function. Lung cancer cells were seeded (1×10^4 cells mL^{-1}) in 100 μL medium/well in 96-well plates, incubated overnight, and treated with various concentrations of BCI for 24 h. Cell viability was calculated by assessing MTS metabolism, as previously reported (Bak et al., 2013). Briefly, media samples (100 μL) were removed and incubated with 100 μL of

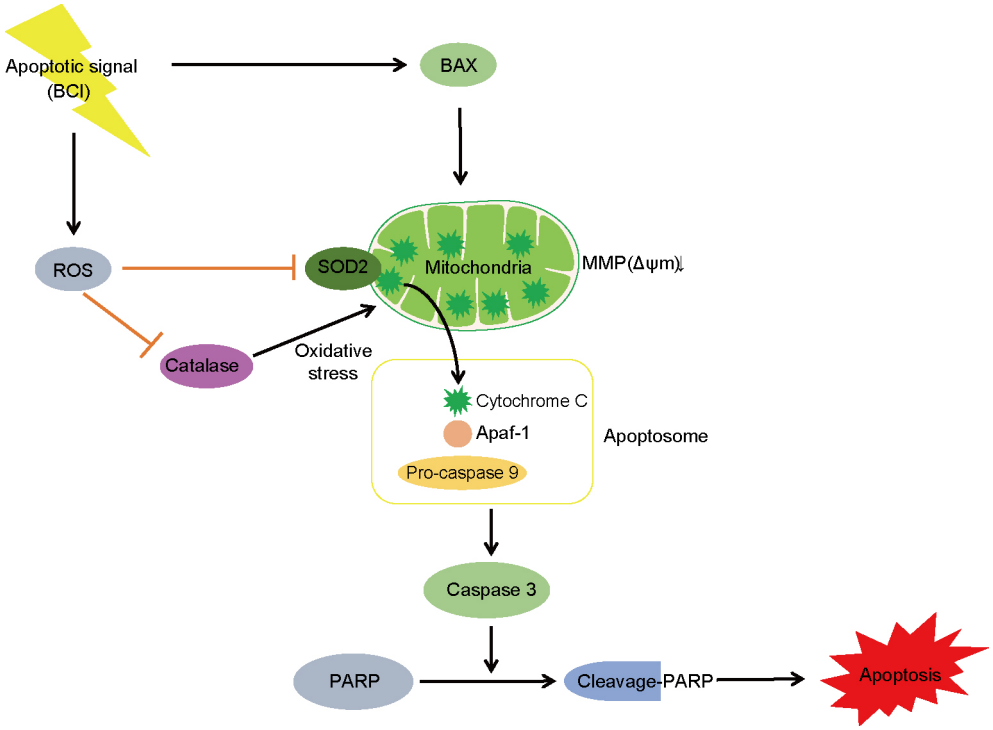

Figure 7 (Color online) Schematic representation of potential BCI-induced apoptotic pathway in NCI-H1299 cells. BCI enhances ROS level, inhibits antioxidant enzymes such as SOD2 and catalase and induces an imbalance between Bcl-2 family proteins such as Bcl-2, Bax, and MMP, leading to apoptosis via intrinsic pathway. BCI also induced processing of caspase-9, caspase-3, and PARP as well as the release of cytochrome c from the mitochondria into the cytosol. In conclusion, BCI induces apoptosis via generation of reactive oxygen species and activation of the intrinsic pathway via induction of an imbalance between Bcl-2 family proteins such as Bcl-2 and Bax in NCI-H1299 cells. The arrows symbolize the activation of the signal pathways; the closed lines symbolize the repression of the signals.

MTS-PMS mix solution for 1 h at 37°C. Optical absorbance was measured at 492 nm wavelength using an enzyme-linked immunosorbent assay reader (Apollo LB 9110, Berthold Technologies GmbH & Co. KG, Germany). *p53* siRNA was purchased from ST pharm (Korea).

Annexin V and PI staining

NCI-H1299 lung cancer cells (1.5×10^5 cells mL^{-1}) were seeded into 60 mm culture dishes and incubated overnight. Cells were treated with BCI for 24 h, harvested using trypsin-ethylenediaminetetraacetic acid (EDTA), and washed with phosphate-buffered saline (PBS). Annexin V and PI staining were performed using FITC-Annexin V apoptosis detection kit I according to the manufacturer's instructions. Data were analyzed by flow cytometry using a FACSCalibur instrument and CellQuest software (BD Biosciences).

Cell cycle analyses by flow cytometry

Cell cycle analysis was performed by PI staining and flow cytometry. NCI-H1299 cells (1.5×10^5 cells mL^{-1}) were seeded into 60 mm culture dishes and treated with various concentrations of BCI for 24 h. Cells were harvested with trypsin-EDTA and fixed with 80% ethanol. Next, the cells were washed twice with cold PBS and centrifuged to discard the supernatant. The pellet was resuspended and stained with PBS containing 50 μg mL^{-1} PI and 100 μg mL^{-1} RNase A for 20 min in the dark. DNA content was analyzed by flow cytometry using a FACSCalibur instrument and CellQuest software.

Western blot analysis

Cells were treated with the specified concentrations of BCI for 24 h, harvested, washed with PBS, and recentrifuged (1,890×*g*, 5 min, 4°C). The resulting cell pellets were resuspended in lysis buffer containing 50 mmol L^{-1} Tris (pH 7.4), 1.5 mol L^{-1} sodium chloride, 1 mmol L^{-1} EDTA, 1% NP-40, 0.25% sodium deoxycholate, 0.1% sodium dodecyl sulfate (SDS), and a protease inhibitor cocktail. The cell lysates were incubated on ice for 1 h and clarified by centrifugation at 17,010×*g* for 30 min at 4°C. Protein content was quantified by the Bradford assay (Bio-Rad, USA) using an UV spectrophotometer. Cell lysates were separated by 12%–15% SDS polyacrylamide gel electrophoresis. Proteins were transferred onto polyvinylidene difluoride membranes (Millipore), which were blocked in 5% non-fat dried milk dissolved in Tris-buffered saline containing Tween-20 (2.7 mol L^{-1} sodium chloride (NaCl), 53.65 mmol L^{-1} potassium chloride (KCl), 1 mol L^{-1} Tris-HCl, pH 7.4, 0.1% Tween-20) for 1 h at room temperature. The membranes were incubated overnight at 4°C with specific primary antibodies. After washing, the membranes were incubated with the secondary antibodies (HRP-conjugated anti-rabbit or anti-mouse IgG) for 1 h at room temperature. The blots were washed and analyzed using West-queen and Western blot detection system (iNtRON Biotechnology, Seongnam, South Korea).

Nuclear and cytoplasmic fractionation

Cells treated with BCI were collected and fractionated using NE-PER nuclear and cytoplasmic extraction reagents (Thermo Fisher Scientific Inc., USA) according to the manufacturer's instruction. Briefly, the treated cells were harvested with trypsin-EDTA and centrifuged at 500×*g* for 3 min. The cell pellet was suspended in 200 μL cytoplasmic extraction reagent I by vortexing. The suspension was incubated on ice for 10 min, followed by the addition of 11 μL of a second cytoplasmic extraction reagent II. The reaction was vortexed for 5 s, incubated on ice for 1 min, and centrifuged for 5 min at 16,000×*g*. The supernatant fraction was transferred to a pre-chilled tube. The insoluble fraction was resuspended in 100 μL nuclear extraction reagent by vortexing for 15 s. The reaction tube was incubated on ice for 10 min and centrifuged for 10 min at 16,000×*g*. The resulting supernatant constituting the nuclear extract was used for the subsequent experiments.

Analysis of MMP

We evaluated MMP ($\Delta\psi m$) by JC-1 staining and flow cytometry. NCI-H1299 cells were seeded into 60 mm culture dishes (1.5×10^5 cells mL^{-1}) and treated with various concentrations of BCI. Cells were harvested with trypsin-EDTA and transferred into 1.5 mL tubes. JC-1 (5 μg mL^{-1}) was added to the cells and mixed until it was completely dissolved, followed by incubation of cells in the dark for 10 min at 37°C in an incubator. The cells were centrifuged (300×*g*, 5 min, 4°C), washed twice with PBS, and resuspended in 200 μL PBS. The solutions were divided using a FACSCalibur instrument and analyzed by Cell Quest software. The protocol was performed in minimal light.

RT-PCR

Cells treated with BCI were harvested. RNA was extracted using an easy-BLUETM total RNA extraction kit (iNtRon Biotechnology, Korea) according to the manufacturer's instructions. cDNA products were obtained using M-MuLV reverse transcriptase (New England Biolabs, USA). Each sample contained one of the following primer sets: *FAS*, 5′-AGGGATTGGAATTGAGGAAG-3′ (forward), 5′-ATGGGCTTTGTCTGTGTACT-3′ (reverse); *TRAIL*, 5′-GTCTCTCTGTGTGGCTGTAA-3′ (forward), 5′-TGTTGCTTCTTCCTCTGGCT-3′ (reverse); *GAPDH*, 5′-GGCTGCTTTTAACTCTGGTA-3′ (forward), 5′-TGGAAGATGGTGATGGGATT-3′ (reverse); *DR5*, 5′-CAGAGGGATGGTCAAGGTCG-3′ (forward), 5′-TGATGATGCCTGATTCTTTGTGG-3′ (reverse); *DR6*, 5′-TGCAGTATCCGGAAAAGCTC-3′

(forward), 5′-TCTGGGTTGGAGTCATGGAT-3′ (reverse); *DR3*, 5′-CTACTGCCAACCATGCCTAG-3′ (forward), 5′-TCGCCATGTTCATAGAAGCC-3′ (reverse); *FADD*, 5′-GGGGAAAGATTGGAGAAGGC-3′ (forward), 5′-CAGATTCTCAGTGACTCCCG-3′ (reverse); *TRADD*, 5′-CTATTGCTGAACCCCTGTCC-3′ (forward), 5′-AGAATCCCCAATGATGCACC-3′ (reverse); *SOD2*, 5′-TATAGAAAGCCGAGTGTTTCCC-3′ (forward), 5′-GGGATGCCTTTCTAGTCCTATTC-3′ (reverse); *catalase*, 5′-GGGATCTTTTAACGCCATT-3′ (forward), 5′-CCAGTTTACCAACTGGATG-3′ (reverse); *peroxiredoxin-1*, 5′-GCTTTCAGTGATAGGGCAGA-3′ (forward), 5′-AAGACCCCATAATCCTGAGC-3′ (reverse); *thioredoxin*, 5′-GAAGCTCTGTTTGGTGCTTTG-3′ (forward), 5′-CTCGATCTGCTTCACCATCTT-3′ (reverse).

Caspase inhibitor assay

The apoptosis mechanism was analyzed using caspase inhibitors. NCI-H1299 cells (1.5×10^5 cell mL^{-1}) were seeded in 60 mm cell culture dishes and treated with 20 μmol L^{-1} pan-caspase inhibitors. After 3 h, 5 μmol L^{-1} BCI was added to each plate. After 24 h, the cells were harvested and used for Western blot analyses.

Detection of intracellular levels of ROS

We used DCF-DA cellular ROS detection assay kit (Abcam, UK) to detect the accumulation of intracellular ROS in NCI-H1299 cells. Briefly, NCI-H1299 cells (2×10^4 cells $well^{-1}$) were seeded into dark 96-well plates and incubated for 24 h. The cells were stained with 25 μmol L^{-1} DCF-DA for 45 min and treated with various concentrations of BCI (0, 1.25, 2.5, and 5 μmol L^{-1}) for 24 h. The fluorescence intensity of each well was quantified with a fluorescence microplate reader (Gemini EM, Molecular Devices, USA) at E_x/E_m=485/538 nm. The experiments were performed at least thrice.

Compliance and ethics *The author(s) declare that they have no conflict of interest.*

Acknowledgements *This work was supported by Konkuk University in 2016.*

Algeciras-Schimnich, A., Pietras, E.M., Barnhart, B.C., Legembre, P., Vijayan, S., Holbeck, S.L., and Peter, M.E. (2003). Two CD95 tumor classes with different sensitivities to antitumor drugs. Proc Natl Acad Sci USA 100, 11445–11450.

Ali, A.G., Mohamed, M.F., Abdelhamid, A.O., and Mohamed, M.S. (2017). A novel adamantane thiadiazole derivative induces mitochondria-mediated apoptosis in lung carcinoma cell line. Bioorg Med Chem 25, 241–253.

Alnemri, E.S., Livingston, D.J., Nicholson, D.W., Salvesen, G., Thornberry, N.A., Wong, W.W., and Yuan, J. (1996). Human ICE/CED-3 protease nomenclature. Cell 87, 171.

Ashkenazi, A. (2008). Targeting the extrinsic apoptosis pathway in cancer. Cytokine Growth Factor Rev 19, 325–331.

Ashkenazi, A., and Dixit, V.M. (1998). Death receptors: signaling and modulation. Science 281, 1305–1308.

Bak, Y., Ham, S., Baatartsogt, O., Jung, S.H., Choi, K.D., Han, T.Y., Han, I.Y., and Yoon, D.Y. (2013). A1E inhibits proliferation and induces apoptosis in NCI-H460 lung cancer cells via extrinsic and intrinsic pathways. Mol Biol Rep 40, 4507–4519.

Bak, Y., Kim, H., Kang, J.W., Lee, D.H., Kim, M.S., Park, Y.S., Kim, J.H., Jung, K.Y., Lim, Y., Hong, J., and Yoon, D.Y. (2011). A synthetic naringenin derivative, 5-hydroxy-7,4′-diacetyloxyflavanone-*N*-phenyl hydrazone (N101-43), induces apoptosis through up-regulation of Fas/FasL expression and inhibition of PI3K/Akt signaling pathways in non-small-cell lung cancer cells. J Agric Food Chem 59, 10286–10297.

Cryns, V., and Yuan, J. (1998). Proteases to die for. Genes Dev 12, 1551–1570.

Dixit, D., Ghildiyal, R., Anto, N.P., and Sen, E. (2014). Chaetocin-induced ROS-mediated apoptosis involves ATM-YAP1 axis and JNK-dependent inhibition of glucose metabolism. Cell Death Dis 5, e1212.

Dixit, D., Sharma, V., Ghosh, S., Koul, N., Mishra, P.K., and Sen, E. (2009). Manumycin inhibits STAT3, telomerase activity, and growth of glioma cells by elevating intracellular reactive oxygen species generation. Free Radic Biol Med 47, 364–374.

Evans, T., Rosenthal, E.T., Youngblom, J., Distel, D., and Hunt, T. (1983). Cyclin: a protein specified by maternal mRNA in sea urchin eggs that is destroyed at each cleavage division. Cell 33, 389–396.

Fulda, S., Galluzzi, L., and Kroemer, G. (2010). Targeting mitochondria for cancer therapy. Nat Rev Drug Discov 9, 447–464.

Han, X., Han, Y., Zheng, Y., Sun, Q., Ma, T., Zhang, J., and Xu, L. (2017). Chaetocin induces apoptosis in human melanoma cells through the generation of reactive oxygen species and the intrinsic mitochondrial pathway, and exerts its anti-tumor activity *in vivo*. PLoS ONE 12, e0175950.

Huang, Y.T., Huang, D.M., Chueh, S.C., Teng, C.M., and Guh, J.H. (2006). Alisol B acetate, a triterpene from *Alismatis rhizoma*, induces Bax nuclear translocation and apoptosis in human hormone-resistant prostate cancer PC-3 cells. Cancer Lett 231, 270–278.

Jemal, A., Bray, F., Center, M.M., Ferlay, J., Ward, E., and Forman, D. (2011). Global cancer statistics. CA-A Cancer J Clin 61, 69–90.

Jeong, S.Y., Han, M.H., Jin, C.Y., Kim, G.Y., Choi, B.T., Nam, T.J., Kim, S.K., and Choi, Y.H. (2010). Apoptosis induction of human leukemia cells by *Streptomyces* sp. Sy-103 metabolites through activation of caspase-3 and inactivation of Akt. Int J Mol Med 25, 31–40.

Karna, P., Gundala, S.R., Gupta, M.V., Shamsi, S.A., Pace, R.D., Yates, C., Narayan, S., and Aneja, R. (2011). Polyphenol-rich sweet potato greens extract inhibits proliferation and induces apoptosis in prostate cancer cells *in vitro* and *in vivo*. Carcinogenesis 32, 1872–1880.

King, K.L., and Cidlowski, J.A. (1998). Cell cycle regulation and apoptosis. Annu Rev Physiol 60, 601–617.

Kischkel, F.C., Hellbardt, S., Behrmann, I., Germer, M., Pawlita, M., Krammer, P.H., and Peter, M.E. (1995). Cytotoxicity-dependent APO-1 (Fas/CD95)-associated proteins form a death-inducing signaling complex (DISC) with the receptor. EMBO J 14, 5579–5588.

Kroemer, G., Dallaporta, B., and Resche-Rigon, M. (1998). The mitochondrial death/life regulator in apoptosis and necrosis. Annu Rev Physiol 60, 619–642.

Kroemer, G., and Reed, J.C. (2000). Mitochondrial control of cell death. Nat Med 6, 513–519.

Lavrik, I., Golks, A., and Krammer, P.H. (2005). Death receptor signaling. J Cell Sci 118, 265–267.

Li, H., Zhu, H., Xu, C., and Yuan, J. (1998). Cleavage of BID by caspase 8 mediates the mitochondrial damage in the Fas pathway of apoptosis. Cell 94, 491–501.

Li, P., Nijhawan, D., Budihardjo, I., Srinivasula, S.M., Ahmad, M., Alnemri, E.S., and Wang, X. (1997). Cytochrome c and dATP-dependent formation of Apaf-1/Caspase-9 complex initiates an apoptotic protease cascade. Cell 91, 479–489.

Li, Z., Xu, X., Huang, Y., Ding, L., Wang, Z., Yu, G., Xu, D., Li, W., and

Tong, D. (2012). Swainsonine activates mitochondria-mediated apoptotic pathway in human lung cancer a549 cells and retards the growth of lung cancer xenografts. Int J Biol Sci 8, 394–405.
Liu, D., Xiao, B., Han, F., Wang, E., and Shi, Y. (2012). Single-prolonged stress induces apoptosis in dorsal raphe nucleus in the rat model of post-traumatic stress disorder. BMC Psych 12, 211.
Lu, J., Bai, L., Sun, H., Nikolovska-Coleska, Z., McEachern, D., Qiu, S., Miller, R.S., Yi, H., Shangary, S., Sun, Y., Meagher, J.L., Stuckey, J.A., and Wang, S. (2008). SM-164: a novel, bivalent smac mimetic that induces apoptosis and tumor regression by concurrent removal of the blockade of cIAP-1/2 and XIAP. Cancer Res 68, 9384–9393.
Mignotte, B., and Vayssiere, J.L. (1998). Mitochondria and apoptosis. Eur J Biochem 252, 1–15.
Molina, G., Vogt, A., Bakan, A., Dai, W., Queiroz de Oliveira, P., Znosko, W., Smithgall, T.E., Bahar, I., Lazo, J.S., Day, B.W., and Tsang, M. (2009). Zebrafish chemical screening reveals an inhibitor of Dusp6 that expands cardiac cell lineages. Nat Chem Biol 5, 680–687.
Moore, A., Donahue, C.J., Bauer, K.D., and Mather, J.P. (1998). Simultaneous measurement of cell cycle and apoptotic cell death. Methods Cell Biol 57, 265–278.
Nagata, S. (2000). Apoptotic DNA fragmentation. Exp Cell Res 256, 12–18.
Pastorino, U. (2010). Lung cancer screening. Br J Cancer 102, 1681–1686.
Rodriguez, J., and Lazebnik, Y. (1999). Caspase-9 and APAF-1 form an active holoenzyme. Genes Dev 13, 3179–3184.
Salvesen, G.S., and Dixit, V.M. (1997). Caspases: intracellular signaling by proteolysis. Cell 91, 443–446.
Sankari, S.L., Masthan, K.M.K., Babu, N.A., Bhattacharjee, T., and Elumalai, M. (2012). Apoptosis in cancer—an update. Asian Pac J Cancer Prevent 13, 4873–4878.
Siegel, R., Naishadham, D., and Jemal, A. (2013). Cancer statistics, 2013. CA-A Cancer J Clin 63, 11–30.
Sipieter, F., Ladik, M., Vandenabeele, P., and Riquet, F. (2014). Shining light on cell death processes—a novel biosensor for necroptosis, a newly described cell death program. Biotech J 9, 224–240.
van Gurp, M., Festjens, N., van Loo, G., Saelens, X., and Vandenabeele, P. (2003). Mitochondrial intermembrane proteins in cell death. Biochem Biophys Res Commun 304, 487–497.
Vermes, I., Haanen, C., Steffens-Nakken, H., Reutelingsperger, C. (1995). A novel assay for apoptosis. Flow cytometric detection of phosphatidylserine expression on early apoptotic cells using fluorescein labelled Annexin v. J Immunol Methods 184, 39–51.
Wilson, N.S., Dixit, V., and Ashkenazi, A. (2009). Death receptor signal transducers: nodes of coordination in immune signaling networks. Nat Immunol 10, 348–355.
Xiao, J.X., Huang, G.Q., Zhu, C.P., Ren, D.D., and Zhang, S.H. (2007). Morphological study on apoptosis Hela cells induced by soyasaponins. Toxicol In Vitro 21, 820–826.
Yang, W.L., Addona, T., Nair, D.G., Qi, L., and Ravikumar, T.S. (2003). Apoptosis induced by cryo-injury in human colorectal cancer cells is associated with mitochondrial dysfunction. Int J Cancer 103, 360–369.

SUPPORTING INFORMATION

Figure S1 Effects of BCI on apoptosis related-factors in NCI-H460 and A549 cells.

Figure S2 Effects of BCI and p53 siRNA in NCI-H460 cells. After transfection of scrambled RNA or p53-targeting siRNA, apoptosis-related factors were analyzed by Western blot analysis in NCI-H460 cells.

The supporting information is available online at http://life.scichina.com and https://link.springer.com. The supporting materials are published as submitted, without typesetting or editing. The responsibility for scientific accuracy and content remains entirely with the authors.